A Joint Risk and Security Constrained Control Framework for Real-Time Energy Scheduling of Islanded Microgrids

Saman Nikkhah, *Graduate Student Member, IEEE*, Ilias Sarantakos, Natalia-Maria Zografou-Barredo, Abbas Rabiee, *Senior Member, IEEE*, Adib Allahham, and Damian Giaouris

Abstract— **High penetration of intermittent renewable energy sources (RES) and unexpected disruptions (e.g., natural disasters) are fundamental challenges which can threaten the secure operation of microgrids, especially during the islanded condition, with no support from the upstream grid. This paper introduces a hierarchical tri-layer min-max-min joint risk- and security-constrained model predictive control (RSC-MPC) framework for real-time energy scheduling of islanded microgrids (IMGs) under the influence of uncertainty and real-time time-varying contingency conditions. While the first layer processes a pre-scheduling day-ahead optimisation, the second layer detects the worst-case contingency conditions by maximising the load curtailment and the mismatch between pre-scheduling (i.e., first layer) and real-time operation. The third layer implements the corrective security measures to minimise the negative effect of contingency conditions while accounting to the cost associated with the risk of uncertainty in the forecasted inputs. The third layer also explores the economic effects of the RES' uncertainty on the proposed RSC-MPC, considering the risk and energy procurement cost as conflicting objectives. The computational efficiency of the proposed hierarchical control system in terms of accuracy and processing time is guaranteed through a mixed integer conic programming model. The proposed RSC-MPC is tested in different case studies and its efficiency is validated by numerical results.**

Index Terms—**Islanded microgrid (IMG), security, risk, conic programming.**

NOMENCLATURE

Indices

i, j	Index of system buses
t/s	Index of time/scenario

Sets

Ω_b	Set of system buses
Ω_b^j	Set of buses that are not connected to the upstream network
Ω_b^s	Set of buses connected to the upstream network
$\Omega_b^{f/c}$	Set of responsive/curtailable loads
$\Omega_{g/w/e}$	Set of DU/WT/ESS installed buses
$\Omega_{t/s}$	Set of time/scenarios

Parameters

$(G/B)_{ij}^{\ell/Sh}$	Series/Shunt conductance/susceptance of the line between buses i and j [pu]
$(P/Q)_{i,\max/min}^G$	Maximum/minimum active/reactive power capacity of DUs [kW]
β	Weighting factor
$\chi_{i,t}^G$	Parameter indicating the on/off status of DUs
Δt	Duration of time periods [hour]
$\eta_i^{Ch/DCh}$	Charge/discharge efficiency of ESS [%]
γ_t^m	Energy price [$/kWh]
π_s^W	The probability of falling to each wind scenario [%]
$\psi_{i,s}^{WT}$	Available wind power at each scenario
ρ	CVaR confidence layer [%]
$I_{\max}^\ell$	Maximum current capacity of branch ℓ [pu]
L_i^{Cur}	Value of loss load [$/kWh]
$P_{i,t,s}^{D_0}$	Base active load [kW]
P_R^{WT}	Rated power of WTs [kW]
$R_i^{U/D}$	Ramp up/down limits of DUs [kW]
RT	Repair time of distribution lines [hour]
$SOC_{\max/min}^{ESS}$	Maximum minimum state of charge of ESS [kWh]
$V_i^{\max/min}$	Maximum/minimum voltage magnitude [pu]

Variables

$(P/Q)_{i,t,s}^D$	Active/reactive load demand [kW/kVAr]
$(P/Q)_{i,t,s}^G$	Active/reactive power output of DUs [kW/kVAr]
$(P/Q)_{i,t,s}^{UN}$	Active/reactive power imported from upstream network [kW/kVAr]
$(P/Q)_{i,t,s}^{WT}$	Active/reactive power output of WTs [kW/kVAr]
$(P/Q)_{ij,t,s}^\ell$	Active/reactive power flow between buses i and j [kW/kVAr]
$(R/T)_{ij,t,s}^\ell$	Variables associated with the line between buses i and j in MICP model [pu]
$\alpha_{ji,t,s}^\ell$	Binary variable specifying the parent bus [=1 if bus i is the parent of bus j, =0 otherwise]
$\beta_{i,t,s}^{res}$	Degree of flexibility of responsive loads [%]
$\lambda_{i,t,s}^{Ch/DCh}$	Binary variables indicating the charge/discharge status of ESS [0,1]
σ	Auxiliary variable indicating the value of CVaR [$]
$\theta_{ij,t,s}$	Voltage angle between buses i and j [pu]
φ_s	Excess of the cost in each scenario over expected cost [$]
$\vartheta_{ij,t,s}^\ell$	Binary variable representing the status of line between buses i and j [0-1]
$P_{i,t,s}^{Ch/DCh}$	Charge discharge power of ESSs [kW]
$P_{i,t,s}^C$	Load curtailment [kW]
$SOC_{i,t,s}^{ESS}$	State of charge of ESS [kWh]
$U_{i,t,s}$	Variable associated with buse i in the MICP model [pu]
$U_{ij,t,s}^\ell$	Variable associated with the line between buses i

i and j in MICP model [pu]

$V_{i,t,s}$ Voltage magnitude of bus i [pu]

I. INTRODUCTION

SECURITY issues have been increasing in power systems in recent years due to the extreme weather events leading to breakdown of infrastructure networks as a result of climate change. On the one hand, more frequent natural disasters have highlighted the necessity of accounting for security measures. On the other hand, increased penetration of volatile renewable generation (to decrease environmental pollution) has created more opportunities, but also challenges for system operators. Therefore, greater share of renewable energy sources (RESs) as well as increased frequency of natural disasters in systems without suitable decentralised control frameworks have provoked substantial challenges to the electricity networks. For instance, the UK power grid outage on August 2019 was the result of high penetration of RESs and the lack of suitable control strategies in the local networks which were disconnected from the main grid by the under-frequency load shedding [1]. Such an event triggered the necessity of designing the microgrids (MGs) that are capable of operating in islanded mode, while accounting for security issues caused by low-probability high-impact contingencies. This operation strategy can prevent, or at least decrease the load shedding of local networks that are disconnected from the main grid.

The islanded operation requires an efficient control mechanism that ensures different operational and physical constraints. Efficient controlling of islanded MGs (IMGs) can enhance the grid reliability and resilience, while improving the RES penetration [2]. Optimal control and energy scheduling of IMGs, however, can be challenged by a wide variety of technical/operational problems. Firstly, due to the inclusion of different inverter-based technologies in the network, the IMG controller should be able to deal with the time-scale discrepancy between the responses of different technologies on a real-time basis. On the other hand, due to the high probability of RES uncertainty, even in a minute-to-minute real-time tracking [3], the risk associated with uncertainty should not be neglected. Therefore, the IMG controller needs to take into account forecasted parameter uncertainty (e.g., in renewable generation) and the potential response delays of different assets in real-time control. Secondly, such a real-time IMG controller should be able to tolerate possible contingency conditions (e.g., a sudden disruption caused by a natural disaster) that can affect grid elements such as distribution system's lines. This problem raises the necessity of accounting for security measures in the IMG's real-time controls. Finally, such control framework should be computationally efficient, while considering important physical and operational constraints of the network.

Several approaches have been proposed in the literature to deal with the aforementioned challenges.

1) Real-time control: Model predictive control (MPC) has been regarded as an efficient approach that is capable of considering system constraints at each time step, enabling real-time control of complex systems. The utilisation of MPC approach in [4] has brought higher RES penetration as well as improvement in the IMG efficiency. In [5] the MPC is adopted to predict future voltage deviations in the IMGs and adjust the reactive power generation to prevent voltage instability. Regardless of the efficiency of MPC-based methods, the main issue in the application of these approaches is the possibility of changes in the predicted data of future time slots. As it has been shown in [6], there is a considerable difference between the actual and predicted photovoltaic generation output, which is caused by the inherent uncertainty of solar irradiance. The effect of RESs uncertainty on the voltage stability of IMGs and optimal capacity of electric vehicle parking lots is analysed in [7]. This factor also has been considered as an important challenge which can affect the system operation [8], load curtailment [9], and system reliability [10]. However, the conventional MPC approaches fail to capture the critical uncertainties (e.g., those associated with RESs) and consequently to handle their associated technical and economic risks. Although it has been considered as the future research work in [4], there is not any research which has investigated the performance of the MPC-based control approaches under an uncertain environment. It should be noted that the effect of uncertainty on the energy management of microgrids has been analysed in recent literature [11], [12], where robust optimisation has been utilised to improve the system robustness in face of uncertainty in the renewable generation. Furthermore, the risk associated with uncertainty of predicted data in the MPC requires more investigation.

2) System security: The occurrence of several natural disasters in recent years [13] obliged system operators to contemplate the contingency conditions as a challenging issue which can affect the power grid [14]. The importance of such constraints in energy management of MGs has been clearly shown in the previous researches [15]–[19], and different preventive and corrective measures have been taken into account to improve the system security. Reference [15] introduced a conservative energy scheduling framework which minimised the dependency on susceptible lines, while concerning the voltage and reactive power constraints as important criteria of secure grid operation. Sun *et al.* [16] proposed a self-healing strategy for MGs to prevent security problems when the grid is facing a contingency condition. The steady state voltage stability of islanded AC-DC MGs with limited reactive power support in the off-grid mode and under the influence of contingencies is studied by [17]. In [18], the security constraints have been integrated into the optimal power flow model in energy management of multi-MGs in a stochastic environment. Contingency conditions have been considered as the main means of defining different security measures [14]. In [19] the role of reserve constraints in providing security margin for isolated microgrids against forecast errors and intra-dispatch fluctuations is analysed by introducing a capacity allocation method. The reserve requirements can be provided by dispatchable units, or optimal management of controllable loads. In [20] optimal management of thermostatically controllable loads is considered as flexibility option for primary frequency regulation. In reality, however, the contingency situations are mainly uncertain phenomena (e.g., natural disasters) that change over a geographical area in a specific period of time. These two factors (i.e., uncertainty in the occurrence of disruptions, and changeability over the system structure) have not been considered in the definition of security.

Network reconfiguration has been regarded as a viable solution to enhance the system security, while keeping a radial structure for the system to facilitate the protection measures. The results obtained in [21] show that the network reconfiguration can change the maximum active droop coefficient through tolerating the impedance. A worst line contingency detection method for the IMGs is proposed in [22], while the mobile

RESs and network reconfiguration are considered as preventive actions to minimise the load curtailment. Application of this method in improving system security is even evident when it has been subjected to different limitations, such as loss-of-load and line capacity constraints [23], or dynamic line rating limitations [24]. A new network reconfiguration in the presence of RESs has been introduced in [25] for post failure system restoration. This method helped in decreasing the costs of restoration program. In [26], the joint optimisation of network reconfiguration and distributed generation is considered as a solution for decreasing the time and cost of system restoration after major faults in the distribution network. The network reconfiguration, however, has been mainly studied as a preventive rather than a corrective measure. Also, the majority of post/pre-reconfiguration problems has been designed based on the known location of faults. However, considering the highly uncertain nature of contingency conditions, changing the system configuration prior to the occurrence of any contingency condition may not influence the elements that will be affected by the event of disruptions.

3) Computational efficiency: Including the security measures in a real-time control mechanism, requires a computationally efficient mathematical model. The existing literature on the real-time energy scheduling of IMGs have mainly adapted mixed-integer nonlinear programming (MINLP) [27] or mixed integer linear programming (MILP) [28] models. Also, those studies which have considered network reconfiguration as a flexibility option for improving the system security have mainly utilised MINLP [22] or MILP [16] models. The main classification criterion for these mathematical methods is the power flow algorithm. Considering a full AC power flow model results in an MINLP problem, and is often solved employing heuristic optimisation methods [29]. However, the MINLP models fail to ensure global optimality (or quantify the optimality gap), while imposing a significant computational burden. The MILP models use some simplifications and approximations in order to linearise the non-convex constraints, which introduce a layer of inaccuracy to model outputs.

The taxonomy of relevant literature on the energy scheduling of IMGs is given in Table I. The studied literature clearly highlighted the importance of including security measures in IMGs operation, as well as the need for using an efficient control mechanism. However, there are several important points in the literature that have not been considered, including: a) importance of security in real-time energy scheduling, b) influence of uncertainty on the real-time operation of system, c) economic factors associated with risk of uncertainty in the real-time energy scheduling, d) real-time flexibility measures created by the energy grid, and e) computational efficiency of a framework that concerns points in (a)-(d). These factors have been highlighted as important research program questions in the Global Power System Transformation (G-PST) Consortium's Research Agenda Group [30]. The relevant questions mentioned in this agenda are [30]:

I. How can operators identify critical stability situations in real-time and optimise system security?

II. How can system operators get relevant real-time visibility and situational awareness of the state of the power system with increasing penetrations of RES and DER?

III. How do control rooms address uncertainties in weather conditions that impact loads and renewable energy output and rate of change (ramps)? How can probabilistic forecasting techniques be better incorporated into real-time operations?

IV. How can grid topology be flexibly adapted at various operating conditions?

In view of the above requirements, this paper proposes a tri-layer min-max-min joint risk- and security-constrained model predictive control (RSC-MPC) framework for real-time energy scheduling of islanded microgrids (IMGs) under the influence of uncertainty and real-time time-varying contingency conditions. The control philosophy starts from first layer cost optimisation, which applies the preventive measures based on the predicted data. The preventive security measures in this layer are adopted through optimal pre-scheduling of DERs, and applying the demand response (DR) program. The second layer aims at identifying the worst-case contingency conditions by maximising the load curtailment and the mismatch between the pre-scheduling energy procurement cost (i.e. first layer) and that of real-time (i.e. second layer). Convex time-varying security constraints are developed for the RSC-MPC controller in the second layer, which consider changeability in the location of disruptions over different zones of the IMG. Finally, in the third layer, the controller develops a convex real-time network reconfiguration as a corrective security measure against the contingency conditions, while re-scheduling the IMG with a trade-off decision making (i.e. making compromise between energy procurement cost and risk of uncertainty in the predicted data). Note that solving the model without the first two layers results in an optimistic decision making which neglects contingency condition or risk of uncertainty. The proposed model benefits from a MICP which is computationally efficient in terms of accuracy and processing time. These developments allow the inclusion of risk and security measures in the real-time energy management of MGs that have to operate in islanded mode. To summarise, the main contributions of this paper are:

- Proposing a multi-layer MICP model for multi-objective energy scheduling of IMGs. The introduced model is computationally efficient and can provide an accurate representation of the power flow model for inclusion in the RSC-MPC.
- Developing a min-max-min RSC-MPC framework which considers the uncertainty of predicted data and the risk associated with them. The introduced control model allows the inclusion of uncertainties in real-time energy scheduling of IMGs while accounting for structural changes in the network topology.
- Building time-varying security constraints based on a MICP power flow model. The proposed framework takes into account the real-time disruptions which change over the grid zones. This framework allows the inclusion of more realistic contingency conditions.
- Developing a corrective real-time network reconfiguration model which improves system security, while guaranteeing the network radiality over uncertainty scenarios (i.e. stochastic network reconfiguration). This framework enables the system controller to change the system configuration so as to prevent load curtailment caused by real-time contingency, while considering the uncertainty.

The remainder of this paper is organised as follows. Overview of the proposed RSC-MPC is given in Section II. The description of different layers and the problem formulation is presented in Section III. Section IV introduces the framework description and case study. Simulation results are given in Section V, while conclusions are summarised in Section VI.

TABLE I: Taxonomy of IMG energy scheduling literature.

Ref. No	Uncertainty	Risk	Constraints		Real-time approach		Reconfiguration		Security measures		Model type
			Security	Reserve	Conventional	Risk-constrained	Normal	Stochastic	Corrective	Preventive	
[4]	x	x	x	✓	✓	x	x	x	x	x	MILP[I]
[5]	x	x	✓	x	✓	x	x	x	x	VVC[II]	MILP
[9]	✓	x	✓	✓	x	x	x	x	x	x	MILP
[14]	x	x	✓	x	x	x	x	x	x	NR[III]	MINLP[IV]
[15]	x	x	✓	x	✓	x	✓	x	DR[V]	NR	MILP
[17]	x	x	✓	✓	x	x	x	x	x	VVC	MINLP
[18]	✓	x	✓	x	x	x	✓	x	x	NR	MINLP
[19]	✓	x	✓	✓	✓	x	x	x	DR	x	MILP
[22]	✓	x	✓	x	x	x	✓	x	x	NR	MINLP
[23]	✓	✓	x	x	x	x	✓	x	x	x	MICP[VI]
[26]	x	x	x	x	x	x	✓	x	NR	x	MILP
This study	✓	✓	✓	✓	x	✓	x	✓	NR	DR	MICP

I: Mixed integer linear programming, II: volt-var control, III: Network reconfiguration, IV: mixed-integer nonlinear programming, V: demand response, VI: mixed-integer conic programming.

II. RISK- AND SECURITY-CONSTRAINED MPC

Using an optimisation-based approach and incorporating the system constraints while also accounting for future timeslots in predicting the state variables are unique advantages of MPC approach, enabling it as a widely-used control mechanism for real-time energy scheduling of IMGs. This controller compiles the optimal control decisions through optimising an objective function for a finite time horizon while only considering the results for the current time interval. For the next timeslot, the controller re-dispatches the system while considering the grid dynamics, past and present control signals. Although such a control framework is efficient in optimising the state variables according to the objective function, it cannot fully address the real-time structural changes in the system topology and the uncertainty of RESs. These challenges reinforce the needs for boosting the efficiency of this control scheme.

The conceptual illustration of the conventional and the proposed MPCs is shown in Fig. 1. In the conventional MPC, the controller dispatches the system for each time interval while considering the whole control horizon. This controller, however, does not account for the uncertainty of RESs, and the risk associated with stochastic generation of these energy sources. For example, when compiling the model at time period $t_{(1)}$, the predicted RES output between time periods $t_{(1+n)}$ and $t_{(1+k)}$ are uncertain and more likely to have different generation scenario from the predicted values. Besides, the occurrence of contingency in the future time intervals cannot be predicted by the conventional control systems. For instance, any disruption between the line connecting the RESs to other parts of the network results in a contingency situation that requires a real-time security measure. Concerning these challenges, this paper introduces a RSC-MPC, which is conceptually illustrated in Fig. 1. This controller accounts for the uncertainty of prediction data, while considering the risk associated with each scenario. Such a risk is defined based on the difference between the expected amount of objective function and its value in different uncertainty scenarios. The proposed RSC-MPC also accounts for real-time contingency condition, while re-dispatches the available sources and upgrades the IMG structure to guarantee the system security.

Note that the proposed method investigates the energy management of an IMG. Therefore, there is no need to optimise the power exchange with the main grid, which requires a tertiary control level [31]. This study performs a MPC-based energy management strategy which is part of secondary control level. It considers the economic aspects of the IMG operation and manages the optimal power flow.
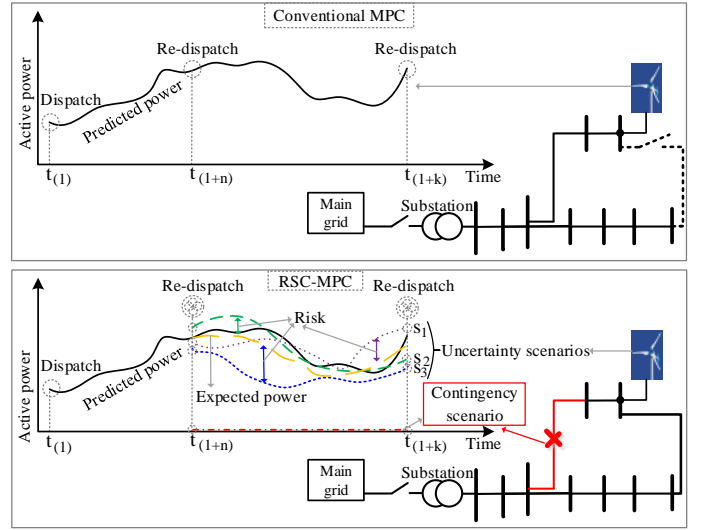

Fig. 1: Comparison of conventional and the proposed MPCs.

III. PROBLEM FORMULATION

Figure 2 illustrates the proposed RSC-MPC framework for IMG energy scheduling, comprising dispatchable units (DUs), and wind turbines (WTs) as the available generation capacity, as well as ESS and DR as the IMG flexibility sources. The proposed architecture is a hierarchical tri-layer min-max-min optimisation. The problem is solved hierarchically with consideration for here-and-now and wait-to-see decision variables. The first layer of the model is a day-ahead scheduling which does not consider MPC and uncertainty scenarios. The second and third layers are MPC-based stochastic optimisation, taking into account contingencies and uncertainty scenarios. The second and third layers are performed on a real-time basis over the control horizon.

The timeline of the each layer is shown in Fig. 3. Considering the availability of weather forecast data on an hourly basis, the second level is solved for one-hour time intervals over the control horizon. Meanwhile, in order to increase the performance and adaptability of the proposed control method to real-time condition [32], the third layer is solved for 5-min time periods.

In the first layer, a pre-scheduling day-ahead cost optimisation is solved so as to determine the preventive measures, consisting of the DER dispatch and the load flow variables (i.e. voltage magnitude/angle of system buses and active/reactive power flow through system branches). These decision variables are obtained for the normal operation of the system and are considered as a reference point for the constraints in second

and third layers. They are used for evaluating the risk of uncertainty and the contingency condition in the real-time operation of the network. The outputs of the first layer are scenario independent (i.e. $X_{i,t,s}^{l1} = X_{i,t}^{l1}$), and considered as here-and-now control actions.

The second layer tries to identify the worst real-time contingency scenarios that can affect the pre-scheduling preventive measures (i.e. the system state in the first layer) under the influence of wind power output uncertainty. The contingency conditions determine the worst line outage scenarios that can affect the normal operation of the system. The optimisation in this layer maximises the mismatch between preventive and real-time actions along with the system load shedding as the objective function, while the location of line-outage scenarios is defined at each time interval on a real-time basis. The decision variables of the second layer (i.e. $X_{i,t,s}^{l2}$) identify the worst contingency scenarios at time period t and the uncertainty scenario s. This information is transferred to the third layer which tries to re-schedule the IMG based on the wort-case scenarios.

The third layer receives the real-time data from the forecast platform and that of previous layers, and re-solves the model to proceed the corrective actions. The corrective decision variables (i.e. $X_{i,t,s}^{l3}$) are preformed by re-dispatching DERs while using the network reconfiguration as a flexibility measure. DER re-dispatching and topology reconfiguration strategies are taken by the third layer at time interval t in face of real-time contingency conditions and the risk associated with uncertainty of wind power prediction at the same time interval. Since the control signals in this layer are proceeded according to the current state of the system in different scenarios, they are identified as the wait-to-see variables (i.e. scenario dependent). At the end of operation horizon, the controller analyses the costs associated with the risk of uncertainty and the security measures. In this section, the mathematical formulation of the proposed MICP stochastic optimisation is presented.

A. Objective function

The mathematical model of the proposed RSC-MPC is built upon an objective function comprised of expected energy procurement cost of IMG, and expected cost of load curtailment, represented by Equation (1). Considering the energy price inside the IMG as a known input [27], the former includes cost of purchasing power from DUs and WTs, the cost of energy arbitrage with the ESS, and the cost of incentivising the responsive loads for participating in the DR program, while the latter represents the load shedding cost based on the value of lost load, as follows:

$$of = \sum_{s \in \Omega_s} \pi_s^W \times \left(C_s^{EP} + C_s^C \right) \quad (1)$$

$$C_s^{EP} = \sum_{t \in \Omega_t} \Delta t \times \gamma_t^m \left\{ \begin{array}{l} \sum_{i \in \Omega_g} P_{i,t,s}^G + \sum_{i \in \Omega_w} P_{i,t,s}^{WT} \\ + \sum_{i \in \Omega_e} \left(P_{i,t,s}^{DCh} - P_{i,t,s}^{Ch} \right) \\ + \sum_{i \in \Omega_b^f} \left(P_{i,t,s}^D - P_{i,t,s}^{D0} \right) \end{array} \right\} \quad (2)$$

$$C_s^C = \sum_{t \in \Omega_t} \sum_{i \in \Omega_b^c} \Delta t \times \left(L_i^C P_{i,t,s}^C \right) \quad (3)$$

where (2) is the energy procurement cost of the IMG in each scenario, in which the first and second terms are respectively costs of purchasing power from DUs and WTs; the third

and fourth terms represent the cost/income of discharging and charging power from/to the ESS respectively; the last term is cost of DR in the responsive loads. Note that the energy price is determined by the upstream network and the microgrid operator tries to minimise the energy procurement cost based on available resources. Equation (3) represents the load curtailment cost at each scenario.

B. Including Risk Constraints in the Objective Function

The first layer of the proposed optimisation is a cost minimisation for here-and-now decision variables. Therefore, the objective function given in (1) is minimised (i.e. $\min \{\Theta^{l1} = of\}$) in this layer. The second layer, however, tries to identify the worst contingency scenarios by maximising the expected load curtailment cost, while maximising the mismatch between the real-time and preventive energy scheduling. This allows the third layer security measures to deal with real-time contingency conditions, and re-dispatch the IMG at each time interval to prevent the security problems that could be the result of energy scheduling mismatch and/or unexpected disruptions. The objective function of the second layer is written as:

$$\max \left\{ \Theta^{l2} = \sum_{s \in \Omega_s} \pi_s^W \times \left((C_s^{EPl2} - C_s^{EPl1}) + C_s^C \right) \right\} \quad (4)$$

The solution obtained in (1), however, is subject to the risk of uncertainty, meaning that it is more likely to observe a considerable difference between expected value of objective function and its individual value in some scenarios. To deal with this risk, several methods have been introduced such as variance, shortfall probability, expected shortfall, value at risk, and conditional value at risk (CVaR). In this study, CVaR is adopted for handling the risk measures due to its advantages, numerical efficiency and stability of calculation for instance, over other techniques [33]. Based on the objective function, the process of including risk measure in the objective function of the proposed RSC-MPC is expressed as:

$$\Re = \sigma - \frac{1}{1-\rho} \sum_{s \in \Omega_s} \varphi_s \pi_s^W \quad (5)$$

$$\left(C_s^{EP} + C_s^C \right) - \sigma \le \varphi_s, \forall s \in \Omega_s \quad (6)$$

where, (5) gives the optimal value of the CVaR (i.e. $\Re$), with $(1-\rho)100\%$ of total cost in each scenario worse than value of VaR (i.e. σ). The difference between expected value and total cost in each scenario is shown by (6), where $\varphi_s \ge 0$.

To consider the risk constraints in the third layer, the expected cost should be increased, based on the value of ρ. In other words, minimising the degree of risk increase the value of energy procurement cost. Under such circumstances, a proper solution can make a trade-off between expense of risk measures and energy procurement cost. To do so, the third layer of the optimisation is solved as multi-objective problem using weighted sum method. Note that the general model is convex and could be solved by different multi-objective handling techniques. Based on this explanation, the general min-max-min objective function of the proposed RSC-MPC is defined as follows:

$$\min \left\{ \begin{array}{l} \beta \times of \left[\max \left(\Theta^{l2} \min \Theta^{l1} \right) \right] \\ + (1 - \beta) \times \Re \left[\max \left(\Theta^{l2} \min \Theta^{l1} \right) \right] \end{array} \right\} \quad (7)$$
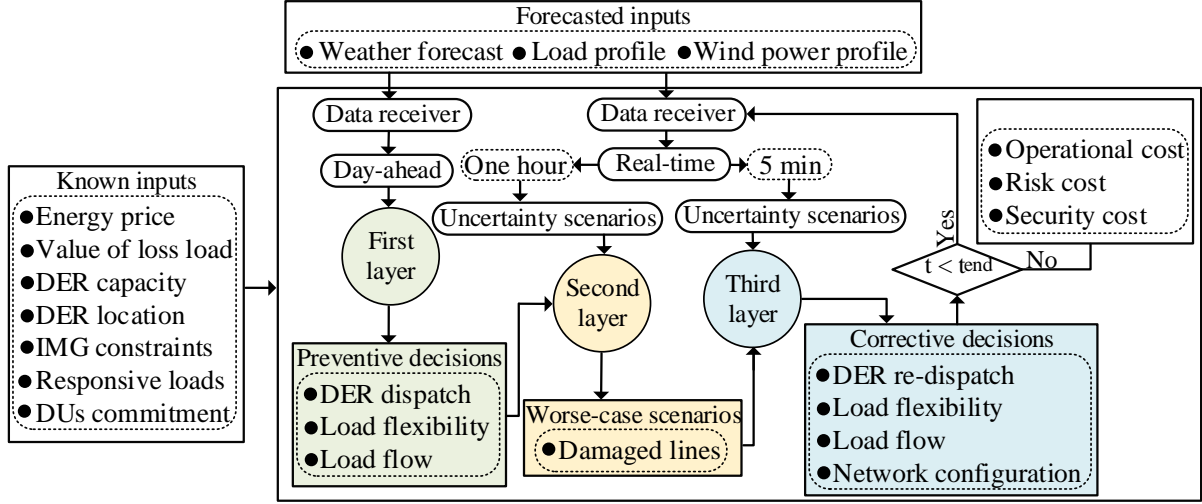
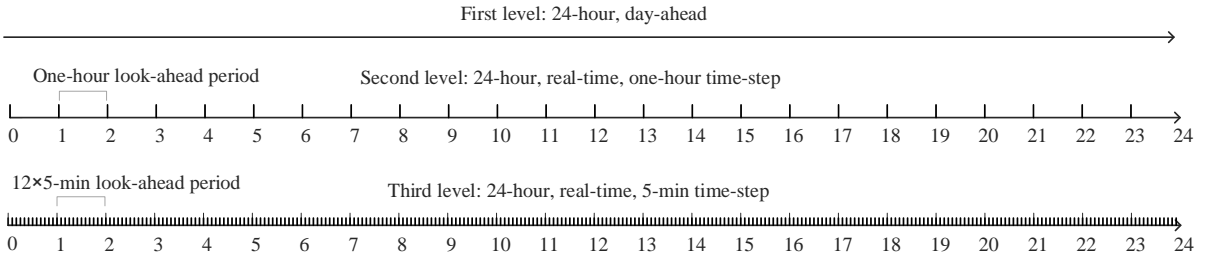Fig. 2: Proposed hierarchical RSC-MPC architecture.

Fig. 3: The proposed RSC-MPC time steps.

C. Power Balance Constraints

The proposed power balance in this study takes into consideration the power output of DUs, WTs, as well as the charge and discharge power of ESS, the participation of responsive loads, and the branch power flow, as follows ($\forall i, j \in \Omega_b, \forall t \in \Omega_t, \ \forall s \in \Omega_s$):

$$P_{i,t,s}^{UN} + P_{i,t,s}^{G} + P_{i,t,s}^{WT} + P_{i,t,s}^{DCh} + P_{i,t,s}^{C} \\ - P_{i,t,s}^{D} - P_{i,t,s}^{Ch} = \sum_j P_{ij,t,s}^{\ell} \tag{8}$$

$$Q_{i,t,s}^{UN} + Q_{i,t,s}^{G} + Q_{i,t,s}^{WT} \\ + \tan\left(\frac{Q_{i,d,t}^{D}}{P_{i,d,t}^{D}}\right) \times P_{i,t,s}^{C} - Q_{i,t,s}^{D} = \sum_j Q_{ij,t,s}^{\ell} \tag{9}$$

$$P_{ij,t,s}^{\ell} = G_{ij}^{\ell} V_{i,t,s}^2 - V_{i,t,s} V_{j,t,s} (G_{ij}^{\ell} \cos\theta_{ij,t,s} + B_{ij}^{\ell} \sin\theta_{ij,t,s}) \tag{10}$$

$$Q_{ij,t,s}^{\ell} = -\left(B_{ij}^{\ell} + \frac{B_{ij}^{Sh}}{2}\right) V_{i,t,s}^2 - V_{i,t,s} V_{j,t,s} (G_{ij}^{\ell} \sin\theta_{ij,t,s} \\ - B_{ij}^{\ell} \cos\theta_{ij,t,s}) \tag{11}$$

where, constraints (8) and (9) represent the real and reactive power injections at each bus, respectively. Constraints (10) and (11) are the real and reactive power flow from bus i to bus j at time step t and scenario s. These constraints, however, are non-convex nonlinear and are more likely to result in a local optimal solution, with a dramatic computation time. On the other hand, linearising the non-linear equations decreases the accuracy of the model. Generally speaking, as mentioned in [34], *"the large boundary is not between linearity and nonlinearity, but between convexity and non-convexity"*. Therefore, a convex relaxation is adopted here by reformulation of continuous variables as follows [35] ($\forall i, j \in \Omega_b, \forall t \in \Omega_t, \ \forall s \in \Omega_s$):

$$U_{i,t,s} = \frac{V_{i,t,s}^2}{\sqrt{2}} \tag{12a}$$

$$R_{ij,t,s}^{\ell} = V_{i,t,s} V_{j,t,s} \cos\theta_{ij,t,s} \tag{12b}$$

$$T_{ij,t,s}^{\ell} = V_{i,t,s} V_{j,t,s} \sin\theta_{ij,t,s} \tag{12c}$$

Therefore, the power flow equations in (10) and (11) are reformulated as follows:

$$P_{ij,t,s}^{\ell} = \sqrt{2} G_{ij}^{\ell} U_{i,t,s} - G_{ij}^{\ell} R_{ij,t,s}^{\ell} - B_{ij}^{\ell} T_{ij,t,s}^{\ell} \tag{13}$$

$$Q_{ij,t,s}^{\ell} = -\sqrt{2}\left(B_{ij}^{\ell} + \frac{B_{ij}^{Sh}}{2}\right) U_{i,t,s} + B_{ij}^{\ell} R_{ij,t,s}^{\ell} - G_{ij}^{\ell} T_{ij,t,s}^{\ell} \tag{14}$$

Variables $R_{ij,t,s}^{\ell}$ and $T_{ij,t,s}^{\ell}$ are new variables that are defined for each line and can be constrained as follows:

$$U_{i,t,s} U_{j,t,s} = \left(R_{ij,t,s}^{\ell}\right)^2 + \left(T_{ij,t,s}^{\ell}\right)^2 \tag{15}$$

This non-convex equation can be relaxed to:

$$U_{i,t,s} U_{j,t,s} \geq \left(R_{ij,t,s}^{\ell}\right)^2 + \left(T_{ij,t,s}^{\ell}\right)^2 \tag{16}$$

Constraint (16) represents the relaxed conic quadratic constraint for branch ij, with free variable $T_{ij,t,s}^{\ell}$ and positive variable $R_{ij,t,s}^{\ell}$. It is worth mentioning that increasing the value of $R_{ij,t,s}^{\ell}$ causes the relaxed inequality constraint in (16) to be binding at optimality [35], which ensures accuracy of the model. This is achieved by minimising the energy procurement cost in (1), leading to the minimisation of net active power injections, which results in an increase of $R_{ij,t,s}^{\ell}$ (since $G_{ij}^{\ell} \geq 0$ in (13)).

D. Distributed Energy Resources

The following constraints represent the capacity and technical limits of different DERs within the IMG, including ESS, WTs, and DUs ($\forall t \in \Omega_t, \forall s \in \Omega_s$):

$$SOC_{i,t,s}^{ESS} = SOC_{i,t-1,s}^{ESS} + \Delta t \left(P_{i,t,s}^{Ch} \eta_i^{Ch} - p_{i,t,s}^{DCh} / \eta_i^{DCh} \right) \\ , \forall i \in \Omega_e \tag{17}$$

$$SOC_{\min}^{ESS} \le SOC_{i,t,s}^{ESS} \le SOC_{\max}^{ESS} \quad , \forall i \in \Omega_e \tag{18}$$

$$0 \le P_{i,t,s}^{Ch} \le \lambda_{i,t,s}^{Ch} P_{\max}^{Ch} \quad , \forall i \in \Omega_e \tag{19}$$

$$0 \le P_{i,t,s}^{DCh} \le \lambda_{i,t,s}^{DCh} P_{\max}^{DCh} \quad , \forall i \in \Omega_e \tag{20}$$

$$\lambda_{i,t,s}^{Ch} + \lambda_{i,t,s}^{DCh} \le 1 \quad , \forall i \in \Omega_e \tag{21}$$

$$0 \le P_{i,t,s}^{WT} \le \psi_{i,s}^{WT} P_R^{WT} \quad , \forall i \in \Omega_w \tag{22}$$

$$-\tan(\varphi_{lead}) P_{i,t,s}^{WT} \le Q_{i,t,s}^{WT} \le \tan(\varphi_{lag}) P_{i,t,s}^{WT} \, \forall i \in \Omega_w \tag{23}$$

$$P_{i,\min}^G \chi_{i,t}^G \le P_{i,t,s}^G \le P_{i,\max}^G \chi_{i,t}^G, \forall i \in \Omega_g \tag{24}$$

$$Q_{i,\min}^G \chi_{i,t}^G \le Q_{i,t,s}^G \le Q_{i,\max}^G \chi_{i,t}^G, \forall i \in \Omega_g \tag{25}$$

$$P_{i,t,s}^G - P_{i,t-1,s}^G \le R_i^U \quad , \forall i \in \Omega_g \tag{26}$$

$$P_{i,t-1,s}^G - P_{i,t,s}^G \le R_i^D \quad , \forall i \in \Omega_g \tag{27}$$

$$\sum_{\forall i \in \Omega_g} \left(\chi_{i,t}^G P_{\max}^G - P_{i,t,s}^G \right) \ge Res_t \tag{28}$$

$$0 \le P_{i,t,s}^C \le P_{i,t,s}^D \quad , \forall i \in \Omega_b^c \tag{29}$$

Constraints (17)-(21) represent the ESS model: (17) shows the state of charge of ESS which is defined based on its value of energy in the previous time period and current state of charge and discharge; (18) limits the upper and lower limit of storage energy; (19) and (20) respectively limit the charge and discharge power; (21) is a logic preventing the simultaneous charge and discharge. Note that ESS can also provide reactive power in Eq. (9). However, it is assumed that the ESSs are operating in unit power factor and only exchange active power with the network, while the reactive power of WTs and DUs is enough to support system demand. The WT active and reactive power is limited by (22) and (23) respectively. Note that the parameter $\psi_{i,s}^{WT}$ represents the available power of WT in Scenario s. Finally, constraints (24)-(27) define the DUs capacity limit, where constraints (24) and (25) show the upper and lower limit of active and reactive power respectively; the ramp up and ramp down limits are applied through (26) and (27) respectively. Constraint (28) shows the reserve requirements at each time interval which is provided by DUs. Consideration of this constraint along with (24) guarantees the provision of reserve requirements. The parameter Res_t is defined by the decision maker which is assumed to be 10% in this study [36]. Finally, Constraint (29) limits the maximum amount of active load that could be curtailed.

E. Demand Response

A certain degree of flexibility is considered for some responsive loads in the system to adjust their consumption based on the electricity price. The load curtailment is also included in the model so as to prevent unrecoverable damages to the IMG in the emergency condition, which helps to keep important security factors (e.g. voltage and frequency)

within acceptable range. The DR programs are introduced as ($\forall t \in \Omega_t, \forall s \in \Omega_s$):

$$(1 - \beta_{i,t,s}^{res}) P_{i,t,s}^{D_0} \le P_{i,t,s}^D \le (1 + \beta_{i,t,s}^{res}) P_{i,t,s}^{D_0}, \forall i \in \Omega_b^f \tag{30}$$

$$\sum_{t \in \Omega_t} P_{i,t,s}^D = \sum_{t \in \Omega_t} P_{i,t,s}^{D_0} \quad , \forall i \in \Omega_b^f \tag{31}$$

$$Q_{i,t,s}^D = \tan \left(\frac{Q_{i,t,s}^{D_0}}{P_{i,t,s}^{D_0}} \right) \times P_{i,t,s}^D \quad , \forall i \in \Omega_b^f \tag{32}$$

where, (30) denotes the maximum and minimum amount of flexibility in the active power demand of responsive loads, while (31) ensures that the total changes in the responsive loads would be equal to the base load by the end of operation period. Constraints (32) represents the changes in the reactive power of responsive loads.

F. IMG Constraints

The branch current, and voltage limits are critical grid constraints which should be satisfied in all layers as follows ($\forall i, j \in \Omega_b, \forall t \in \Omega_t, \forall s \in \Omega_s$):

$$\left(I_{ij,t,s}^\ell \right)^2 = \sqrt{2} \left(\left(G_{ij}^\ell \right)^2 + \left(B_{ij}^\ell \right)^2 \right) \\ \times \left(U_{i,t,s} + U_{j,t,s} - \sqrt{2} R_{ij,t,s}^\ell \right) \le \left(I_{\max}^\ell \right)^2 \tag{33}$$

$$\frac{\left(V_i^{\min} \right)^2}{\sqrt{2}} \le U_{i,t,s} \le \frac{\left(V_i^{\max} \right)^2}{\sqrt{2}} \tag{34}$$

where constraint (33) shows the squared current of branch ij as a linear equation. Also, voltage magnitude is limited by (34).

G. Time-varying Security Constraints

Unexpected disruptions can change the structure of the MGs dramatically, and cause serious security issues, especially during the islanded operation. According to [37], most of the failures in the electrical network are related to weather events, while the majority of these events affect the distribution networks. Given a wide variety of weather events, this paper concerned about high winds and their impact on the security of MGs. The contingency scenario is referred to as a high intensity wind which can cause damage to the overhead lines, such as storm Malik and storm Corrie in the UK [38]. The overhead lines are considered to be the most susceptible elements of the network. Considering the fact that these storms affected parts of Europe and UK from hours to days, the control horizon of 24 hours is assumed as the duration of the weather event. Considering a synoptic wind which is a large moving pressure with a horizontal effect over hundreds of kilometers [39], a set of time-varying security constraints are introduced in the proposed RSC-MPC model, which change over the IMG zones and are influenced by the uncertainty of wind power generation. The term 'time-varying' refers to the real-time changeability of disruption over the operation horizon at each time interval. As opposed to the previous studies which have considered known locations for the damaged elements of the system, the proposed method defines the location of fault at each time interval on a real-time basis.

While a non-linear model multiplies a binary variable into the active and reactive power flow constraints [22], this study introduces variables $U_{ij,t,s}^\ell$ and $U_{ji,t,s}^\ell$ for identifying the status of branches, as follows ($\forall i, j \in \Omega_b, \forall t \in \Omega_t, \forall s \in \Omega_s$):

$$0 \leq U_{ij,t,s}^{\ell} \leq \frac{(V_i^{\max})^2}{\sqrt{2}} \vartheta_{ij,t,s}^{\ell-} \qquad (35)$$

$$0 \leq U_{ji,t,s}^{\ell} \leq \frac{(V_j^{\max})^2}{\sqrt{2}} \vartheta_{ij,t,s}^{\ell-} \qquad (36)$$

$$0 \leq U_{i,t,s} - U_{ij,t,s}^{\ell} \leq \frac{(V_i^{\max})^2}{\sqrt{2}} (1 - \vartheta_{ij,t,s}^{\ell-}) \qquad (37)$$

$$0 \leq U_{j,t,s} - U_{ji,t,s}^{\ell} \leq \frac{(V_j^{\max})^2}{\sqrt{2}} (1 - \vartheta_{ij,t,s}^{\ell-}) \qquad (38)$$

$$\vartheta_{ij,t,s}^{\ell-} = \vartheta_{ji,t,s}^{\ell-} \qquad (39)$$

$$\sum_{ij \in \Omega_b^z} \frac{\left(1 - \vartheta_{ij,t,s}^{\ell-}\right)}{2} = \Im_z \ , \forall t \in \Omega_t^z \qquad (40)$$

$$\frac{\sum_t^{t^r} \left(\Delta t \times \vartheta_{ij,t,s}^{\ell-}\right)}{RT} \leq 1 \qquad (41)$$

where constraints (35)-(38) represent the branch connection status, based on variables $U_{ij,t,s}^{\ell}$ and $U_{ji,t,s}^{\ell}$. These variables take the values of $U_{i,t,s}$ or $U_{j,t,s}$, if the branch is closed (i.e. $\vartheta_{ji,t,s}^{\ell-} = 1$), and are set to zero, if the branch is open (i.e. $\vartheta_{ji,t,s}^{\ell-} = 0$). Therefore, $\vartheta_{ji,t,s}^{\ell-}$ is suggested in this paper for identifying the location of disruption in the IMG. Constraint (40) indicates the occurrence of a specific number of disruptions in each zone (i.e. $\Im_z$) over the period of time at which the zone is experiencing contingency condition (i.e. Ω_t^z), based on the set of buses located in each zone (i.e. Ω_b^z). Finally, constraint (41) ensures that the damaged line is out-of-service for time periods t $\in$ [t, t+t^r], where t$^r = \left(\frac{1}{\Delta t}\right) \times RT$. The proposed constraints in (35)-(41) are adaptable with the proposed MICP power flow model, and are a novel characteristic of the introduced convex security-constrained optimisation model. By introducing variables $U_{ij,t,s}^{\ell}$ and $U_{ji,t,s}^{\ell}$ there is a need to modify equations (13), (14), and (16), as below:

$$P_{ij,t,s}^{\ell} = \sqrt{2} U_{ij,t,s}^{\ell} G_{ij}^{\ell} - G_{ij}^{\ell} R_{ij,t,s}^{\ell} - B_{ij}^{\ell} T_{ij,t,s}^{\ell} \qquad (42a)$$

$$Q_{ij,t,s}^{\ell} = -\sqrt{2} \left(B_{ij}^{\ell} + \frac{B_{ij}^{Sh}}{2}\right) U_{ij,t,s}^{\ell} + B_{ij}^{\ell} R_{ij,t,s}^{\ell} - G_{ij}^{\ell} T_{ij,t,s}^{\ell} \qquad (42b)$$

$$U_{ij,t,s}^{\ell} U_{ji,t,s}^{\ell} \geq \left(R_{ij,t,s}^{\ell}\right)^2 + \left(T_{ij,t,s}^{\ell}\right)^2 \qquad (42c)$$

$$\left(I_{ij,t,s}^{\ell}\right)^2 = \sqrt{2} \left(\left(G_{ij}^{\ell}\right)^2 + \left(B_{ij}^{\ell}\right)^2\right) \times \left(U_{ij,t,s}^{\ell} + U_{ji,t,s}^{\ell} - \sqrt{2} R_{ij,t,s}^{\ell}\right) \leq \left(I_{\max}^{\ell}\right)^2 \qquad (42d)$$

The variables $U_{ij,t,s}^{\ell}$ and $U_{ji,t,s}^{\ell}$ which identify the status of branch ij, equal to $U_{i,t,s}$ and $U_{j,t,s}$, respectively, in normal situation (before occurrence of any disruption). These constraints are defined based on the status of lines connecting buses. Therefore, they are solved for each time step over the operation horizon on a real-time basis.

H. Corrective Security Measures

Several methods have been introduced in the literature to respond to the contingency conditions. Among those methods, network reconfiguration has been regarded as an effective solution in improving the system security [21]. This method can prevent load curtailment in a contingency condition while

ensuring the radiality of the network. In the previous literature [15], [24], however, the network radiality constraints are adopted based on the graph theory (i.e. number of lines=number of buses-1). Although this constraint is necessary condition for the reconfiguration, it cannot guarantee radiality. Besides, this method has been considered as a preventive measure, rather than a real-time action that can deal with unexpected real-time contingency conditions, while taking the uncertainty into account. To deal with this issues, a new convex model is introduced in this study to guarantee secure load supply within the IMG after occurrence of disruptions (i.e. equations (35)-(40)), while keeping the radial configuration of the system in an uncertain environment. A binary variable (i.e. $\vartheta_{ij,t,s}^{\ell+}$) is introduced to correct the possible damage caused by the contingency binary variable (i.e. $\vartheta_{ij,t,s}^{\ell-}$). Also, network radiality for an IMG is achieved by ensuring that the characteristic of spanning trees holds true, meaning that every node has exactly one parent. Therefore, the proposed method in this paper is a stochastic network reconfiguration which operates as a corrective real-time measure in the IMG. Note that the high-frequency reconfiguration is considered as a practical measure since only some specific switches actively participate in the process [40]. Based on this explanation, the branch connection constraints are reformulated as follows ($\forall i, j \in \Omega_b, \forall t \in \Omega_t, \ \forall s \in \Omega_s$):

$$0 \leq U_{ij,t,s}^{\ell} \leq \frac{(V_i^{\max})^2}{\sqrt{2}} (\vartheta_{ij,t,s}^{\ell+} + \vartheta_{ij,t,s}^{\ell-}) \qquad (43)$$

$$0 \leq U_{ji,t,s}^{\ell} \leq \frac{(V_j^{\max})^2}{\sqrt{2}} (\vartheta_{ij,t,s}^{\ell+} + \vartheta_{ij,t,s}^{\ell-}) \qquad (44)$$

$$0 \leq U_{i,t,s} - U_{ij,t,s}^{\ell} \leq \frac{(V_i^{\max})^2}{\sqrt{2}} \left(1 - (\vartheta_{ij,t,s}^{\ell+} + \vartheta_{ij,t,s}^{\ell-})\right) \qquad (45)$$

$$0 \leq U_{j,t,s} - U_{ji,t,s}^{\ell} \leq \frac{(V_j^{\max})^2}{\sqrt{2}} \left(1 - (\vartheta_{ij,t,s}^{\ell+} + \vartheta_{ij,t,s}^{\ell-})\right) \qquad (46)$$

$$\vartheta_{ij,t,s}^{\ell+} + \vartheta_{ij,t,s}^{\ell-} \leq 1 \qquad (47)$$

$$\vartheta_{ij,t,s}^{\ell+} = \vartheta_{ji,t,s}^{\ell+} \qquad (48)$$

$$\alpha_{ij,t,s}^{\ell} + \alpha_{ji,t,s}^{\ell} = (\vartheta_{ij,t,s}^{\ell+} + \vartheta_{ij,t,s}^{\ell-}) \qquad (49)$$

$$\sum_{j \in \Omega_i^j} \alpha_{ij,t,s}^{\ell} = 1 \qquad (50)$$

$$\alpha_{ij,t,s}^{\ell} + \alpha_{ji,t,s}^{\ell} = 0 \qquad , \forall i \in \Omega_b^s \qquad (51)$$

Constraints (43)-(46) represent the branch connection status based on the binary variable indication the disruption (i.e. $\vartheta_{ij,t,s}^{\ell-}$) and the binary variable that corrects the system configuration (i.e. $\vartheta_{ij,t,s}^{\ell+}$). Since it is not practically possible to repair the damaged line at time period t in a real-time paradigm, constraint (47) is introduced to arrange the new system configuration at time period t with consideration for the disruption on a real-time basis. In addition, constraints (49)-(51) ensure the network radiality after applying the corrective actions. Constraint (49) shows that the branch ij is in the spanning tree, if one node is the parent of the other. Constraint (50) indicates that each bus must have exactly one parent. For an IMG, the status of the line connecting the grid to the upstream network is open. Therefore, the slack bus is not parent node to any buses and vice versa. This has been modelled by Constraints (51).

Note that this study investigates a case of contingency in a grid-connected MG. Therefore, the right-hand side of constraint (51) is equal to zero, indicating the islanded operation of MG. The storage units and load shedding capability can be utilised in an IMG for preventing the voltage and frequency excursion. This formulation is different for an isolated MG. In this type of grid, there is no point of common coupling between MG and the upstream grid, and it operates permanently in stand alone mode [31]. Therefore, the variables indicating the power exchange with the main grid in constraints (8) and (9) (i.e. $P_{i,t,s}^{UN}$ and $Q_{i,t,s}^{UN}$)are neglected. Also, there is no need to define constraint (51) in an isolated MG. The voltage and frequency control in an isolated MG is more strenuous task.

IV. FRAMEWORK DESCRIPTION AND CASE STUDIES

This section summarises the solution framework for the proposed RSC-MPC, and provides information on the test system and data utilised for validating the model.

A. Framework Description

The framework of implementing the mathematical model (given in Section III) on the proposed RSC-MPC architecture is sketched in Fig. 4. At the core of this framework, the predicted data is received. Then, the first layer optimisation is processed, where the energy procurement cost is minimised to produce here-and-now decision variables. The MG is in its normal condition and there is no change in the configuration of the system, i.e., without consideration for constraints (35)-(51). Note that it is assumed the MG is self-sustainable, with adequate DER capacity to supply the demand in the normal condition; therefore, load curtailment is not expected in the first layer. The information obtained from this layer is utilised to evaluate the security measures and the consequences of mismatch between the predicted and real-time data along with the risk associated with uncertainty of renewable power generation. Therefore, as a multi-layer optimisation, other layers are optimised with regard to the information processed in the first layer, including the energy procurement cost. Although different sources of uncertainty (e.g. energy price, system load) and various assets (e.g. photovoltaic, micro-hydro) can be considered in the definition of the problem, the main focus of this study is on the effect of uncertainty on the MPC-based real-time energy management methods. Therefore, no uncertainty has been considered in the forecast of other input data and wind power generation is taken into account as the only uncertain input. The second layer tries to detect the worst real-time line contingency scenarios in the system, and maximise the mismatch between real-time IMG dispatch and that of pre-scheduling. The output of this layer is considered as a security constraint for the inner layer, to be corrected at each time interval of operation horizon. Therefore, the third layer's optimisation is processed subject to the unavailability of critical lines and the mismatch between real-time and pre-scheduled data. Also, constraint (51) is considered in this layer, meaning that the microgrid experience an islanded mode after a contingency condition. Since the third layer tries to minimise the cost associated with risk of uncertainty, the energy procurement cost is more likely to rise. Therefore, the third layer optimisation tries to make a trade-off between energy procurement cost and the expense of dealing with the risk of exceeding the expected cost. Without the first two layers, the model would be solved in an optimistic manner and can not tolerate any contingency condition or risk
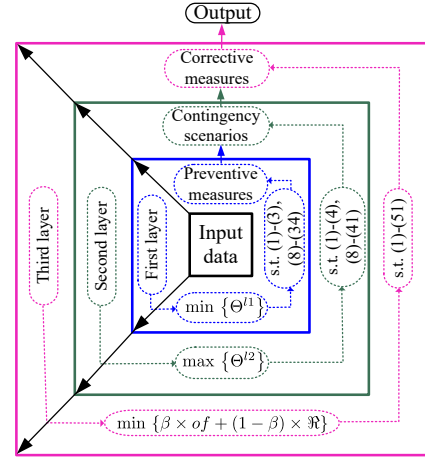

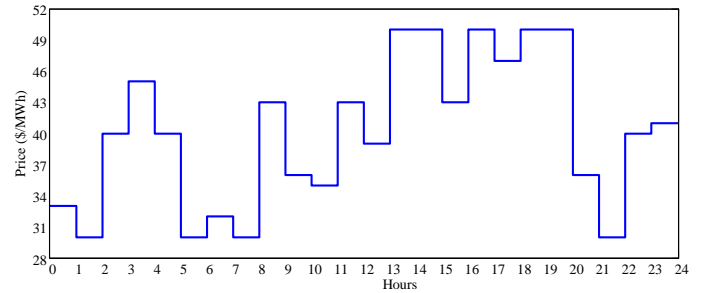Fig. 4: The framework of solving the proposed model.

Fig. 5: Day-ahead energy price signals.

of uncertainty. It is assumed that cloud computing enables the real-time communication, while observing privacy and reliability of communication.

B. Case Studies

The proposed MICP model is executed in general algebraic modelling system (GAMS) using MOSEK solver. The IEEE 33-bus test system is adapted as the test MG, with 5 tie switches that are considered at the third layer as the means of corrective measures. The data of the system under study is taken from [41]. The day-ahead energy price profile is given in Fig. 5. Therefore, the proposed multi-period optimal power flow model in this paper is solved following a UC which defined the ON/OFF status of DUs. Since the paper investigates the real-time security issues in an emergency condition, it has only focused on the the proposed three-layer framework through the proposed AC optimal power flow model. Therefore, the commitment status of DUs is considered as an input parameter in Fig. 2. The islanded operation of the system is guaranteed based on (45). The one-line diagram of the test system, with the location of DERs, curtailable and responsive load buses, along with the operation horizon of the control system are illustrated in Fig. 6. It is assumed that distribution lines are located in three different zones, shown with different colours in Fig. 6. The lines located in each zone are assumed to be in a close geographical location in the IMG. An operation horizon of 24 hours with respectively one-hour and 5-min time steps for the second and third layers is considered for the controller. Note that the majority of weather forecast or natural disaster tracking platforms are working on an hourly basis. Since the second layer of the simulation captures the effects of contingency (caused by natural disaster) on the operation of the microgrid, one-hour time intervals are considered for this layer. Meanwhile, to
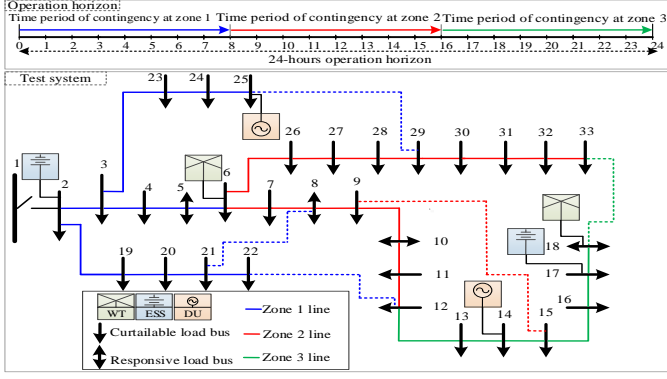
Fig. 6: Schematic diagram of the test IMG, and the operation horizon.

TABLE II: Wind power output uncertainty scenarios.

Scenario number	$\psi_{i,s}^{WT}$ [%]	π_s^W
s_1	0.0	0.069
s_2	12.9	0.204
s_3	49.4	0.404
s_4	86.8	0.199
s_5	100	0.123

increase the performance and adaptability of the system to real-time conditions the third layer is solved for 5-min time steps.

Considering a 9.85 MVA conductor with R = 0.259 Ω/km, it can be derived that the total length of the IEEE 33-bus network is approximately 80 km. Considering a synoptic wind which passes with a horizontal effect over hundreds of kilometers, it is assumed the weather event moves translational speed over a 24 hours. Therefore, the duration of the high wind at each zone of the system is assumed to be 8 hours. It is assumed that the overhead lines are the most susceptible elements of the IMG. Two hours of repair time is considered for each branch [42], while assuming that additional manpower and resources are prepared for the event of storm. Also, the network reconfiguration is considered on hourly basis.

The rated capacity of WTs is considered to be 1000 kW, while the minimum and maximum output of DUs is assumed to be 500 kW and 1500 kW respectively. The storage capacity, and charge/discharge power is 1000 kWh, and 200 kW respectively, with the battery efficiency of 90%. The maximum flexibility of responsive loads is assumed to be 15%, and the value of loss load is assumed to be 10 $\$/kWh$. The power output of the WTs is considered as the source of uncertainty in the system. Five uncertainty scenarios are generated for the wind power uncertainty, using historical data and scenario-based method. Uncertainty scenarios are generated according to [7]. The wind power output scenarios are summarised in Table II.

Various aspects of the model are examined through the following case studies:

Case I: The model is solved without consideration for risk of uncertainty, and security constraints (i.e. neglecting constraints (35)-(51)). This case is equivalent to conventional MPC models.

Case II: The model is solved with consideration for security measures, while neglecting the risk of uncertainty (i.e. $\beta = 1$ in (7)). The case is also called risk neutral (RN).

Case III: Risk and security are the main concern of the controller in this case and the decisions are made without considering the economic consequences (i.e. $\beta = 0$ in (7)).
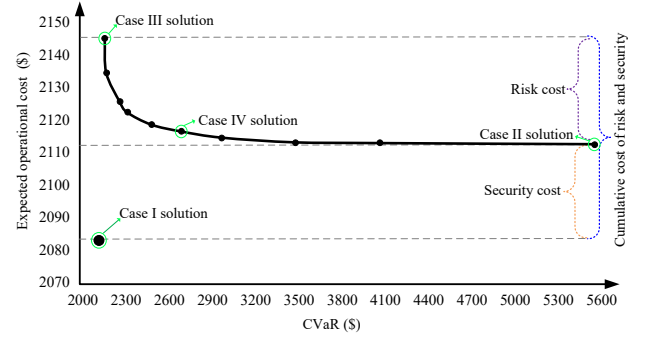

Fig. 7: Value of cost and CVaR in different case studies.

The solution of this case is called risk averse (RA).

Case IV: The controller makes a trade-off between cost associated with risk of uncertainty, security measures and the energy procurement cost.

V. SIMULATION RESULTS

In the following, the important aspects of the model are evaluated based on different case studies, while the performance of the model is further demonstrated by sensitivity analyses and computational statistics.

When the system is operating in a normal condition, any intentional or unintentional disruptions can affect its performance, requiring the IMG operator to take corrective measures. Rescheduling the system under such circumstances, however, is more likely to impose additional costs to the IMG operator. Figure 7 illustrates the Pareto optimal front of the CVaR and the energy procurement cost in different case studies. This figure provides the economic figures for different case studies of the proposed RSC-MPC. The solutions of the Pareto set vary from a RN (i.e. *Case II*) to a RA (i.e. *Case III*). The difference between the cost of these cases is considered as the expense of accounting for the risk associated with uncertainty. Also, the difference between cases I and II is the security cost. Accordingly, with a cumulative cost of $62.12, the MG operator paid $32.50, and $29.62 for dealing with risk and security respectively. These costs should be considered in the energy management of the MGs that are more prone to contingency and are under the penetration of RESs. To make a trade-off between RN and RA solutions, the best compromise solution is obtained in *Case IV*, as shown in Fig. 7.

In order to analyse the performance of CVaR measure in handling the risk of uncertainty scenarios in the real-time energy scheduling, the energy procurement cost of each scenario in *Case II*, and *Case III* along with that of *Case IV* is depicted and compared with the expected cost of each strategy in Fig. 8. The red bars show the scenarios in which the energy procurement cost exceeded the expected cost (i.e. blue bar), while the green bars stand for the scenarios with lower/equal energy procurement cost than/to the expected value. These figures show how risk of uncertainty can influence the real-time energy scheduling over different scenarios. For the RN solution (i.e. *Case II*), it is shown that the energy procurement cost in all scenarios is higher than the expected cost. However, the CVaR measure decreased such a gap between solutions of different scenarios in the RA strategy (i.e. *Case III*). Consequently, the expected cost is increased by $32.50. Finally, the compromise solution (i.e. *Case IV*), made a trade-off between these two cases, as shown in Fig. 8. The security constraints and risk measures are compensated by the energy procurement cost of $62.12 compared to *Case I*.
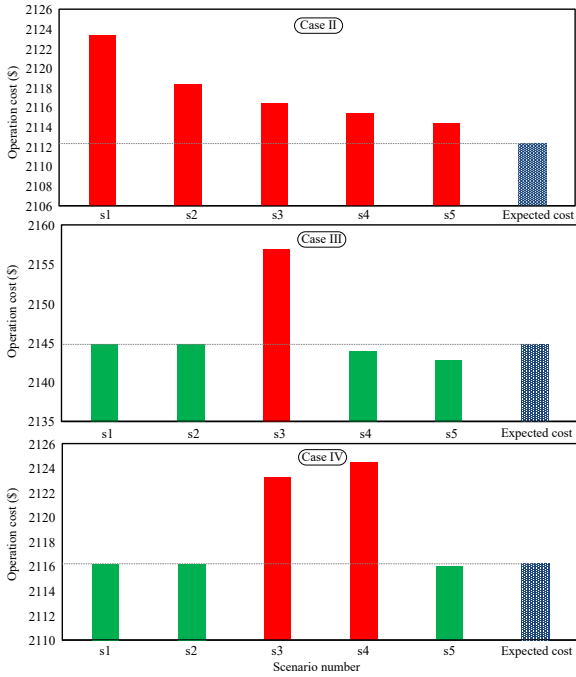
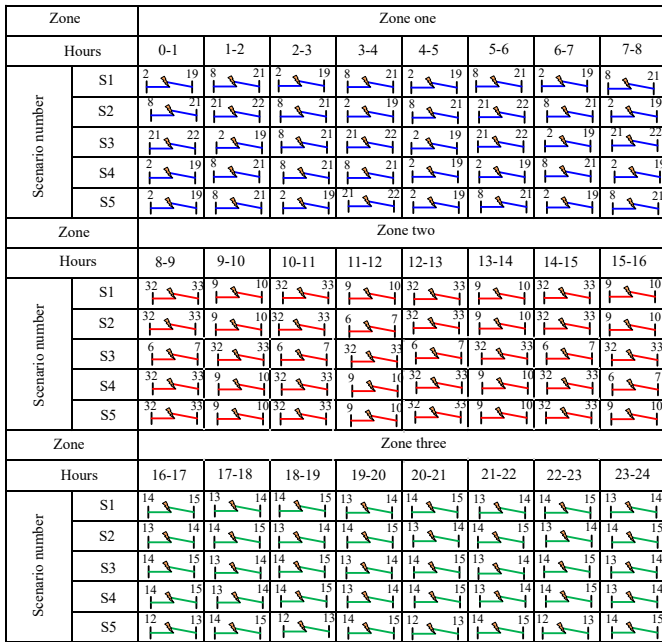Fig. 8: Application of CVaR in decreasing the energy procurement cost.

Fig. 9: Variation of real-time contingency conditions.

Figure 9 shows the result of worst-case line contingency conditions based on the proposed method in equations (35)-(41), for each zone of the MG in different uncertainty scenarios. The repair time is considered to be two hours. Therefore, a failed line at time-period t remained out-of-service until time period $t+2$. The vulnerable lines are mainly recognised around the DERs; especially WTs as their output power change in each scenario. The changes in the uncertainty scenarios affected the classification of worst-case scenarios. Considering the fact that high winds can increase the WT's generation, the worst-case line outages in Scenario s_5 (i.e. high wind power generation) should be considered as the most critical lines for the MG.

However, the corrective measures taken in the third layer prevented load curtailment by employing topology reconfiguration on a real-time basis. Variation in the hourly status of the
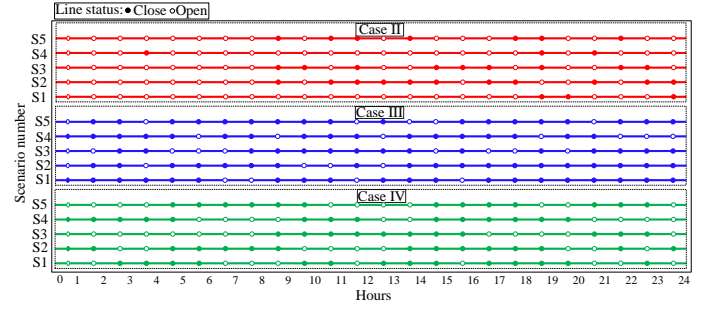

Fig. 10: The corrective configuration of line between buses 8 and 9 in different case studies.

line between buses 8 and 9 in different real-time uncertainty scenarios over system zones is depicted in Fig. 10. Knowing that this line is one of the longest lines in the network (i.e. with a high resistance), in the RN strategy (i.e. *Case II*), it is mostly open while it has been changed to closed status in the RA strategy *Case III*. Opening this line decreases the power loss, and consequently the energy procurement cost. However, in the latter case, this line is a strategic connection between two buses that direct the flow of power to different parts of the network and can comply with the deviation of WT power output (Fig. 6). Similar to the energy procurement cost, the compromise solution in *Case IV* considered a trade-off between RN and RA strategies. Generally, if the economic issues are important to the IMG operators, the compromise solution can be a case with a lower cost and some degree of risk aversion.

The decisions made by the IMG operator regarding the inclusion of risk and security measures can affect the optimal scheduling of energy resources, as shown in Fig. 11. The optimal scheduling of available energy resources in scenarios with no wind power generation (i.e. s_1) and high wind power generation (i.e. s_5) is depicted in this figure. It can be seen that the injected power of WT in RN strategy is more than that of RA. This means that the decision maker needs to decrease the WT output power to deal with the risk of uncertainty. On the other hand, to deal with such a risk, there is a need to use more reliable units such as DUs. Therefore, the power output of DUs in scenario s_5 for the RA strategy is more than that of the RN. Besides, in the scenarios with no wind (i.e. s_1), the participation of DUs in load supply is more obvious, which shows the importance of these units in boosting the system security. To deal with variation of load, the ESS played its part by charging in off-peak periods and discharging during peak hours. Finally, the responsive loads consumption pattern is adjusted accordingly to deal with load variation and electricity price signals.

In order to show the effect of higher layer decisions on the final solutions of the inner layer optimisation, a freedom level (e.g. ΔX_l^{dv}) is introduced to the decision variables transferred from each layer to another. ΔX_l^{dv} indicates the level of freedom between the linking decision variables transferred between the layers. For example $\Delta X_l^{dv} = 15\%$ means that the linking decision variables have 15% degree of freedom, i.e. $(1-0.15) \times \Delta X_l^{dv^H} \leq \Delta X_l^{dv^L} \leq (1+0.15) \times \Delta X_l^{dv^H}$; where $\Delta X_l^{dv^H}$ stands for decision variables of higher layers (i.e. layer one) and $\Delta X_l^{dv^L}$ shows the inner layer decision variables (i.e. second layer). Figure 12 demonstrates the variation of CVaR and expected cost in RA strategy over risk aversion degree (i.e. ρ) for different values of freedom in the linking decision variables. It is shown that increasing the risk aversion degree
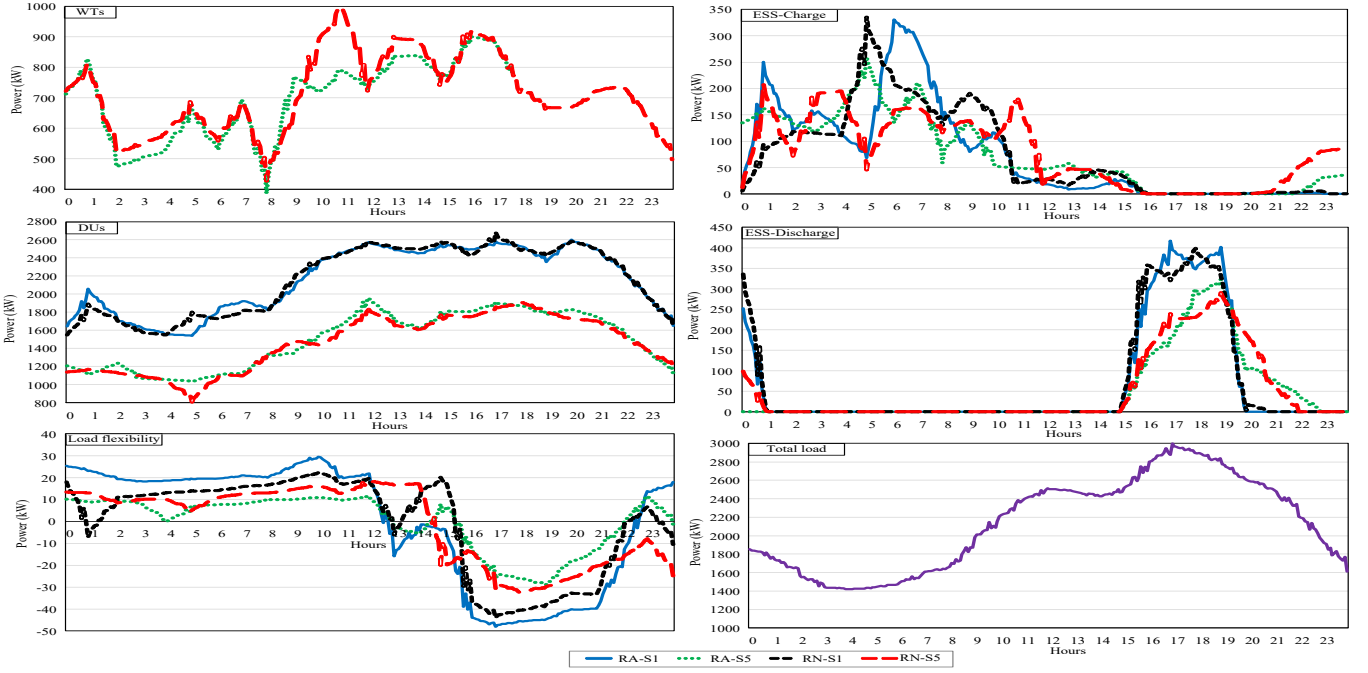
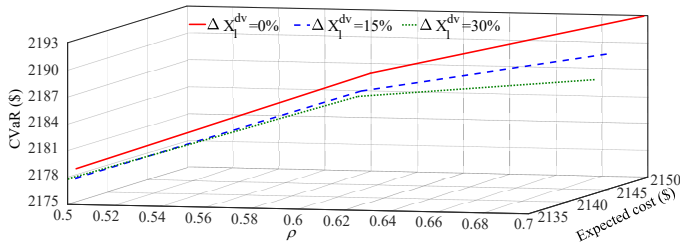Fig. 11: Optimal scheduling of different DERs in different cases.

Fig. 12: Variation of CVaR and expected cost over the changes in the risk aversion degree.

TABLE III: Computational data of the proposed MICP model.

Parameter	Value
Number of single variables	1,404,506
Number of iterations	22,239
Execution time [s]	1,893.6
Relative gap	0.002

raises the cost of dealing with the risk of uncertainty. Besides, it can be seen that the optimal values of CVaR and expected cost have not experienced a dramatic change when the degree of freedom is increased. For example, introducing 15% degree of freedom for $\rho = 0.5$ resulted in 0.01% and 0.05% changes in the values of expected cost and CVaR respectively, while it brought about 0.22% and 0.14% for $\rho = 0.7$ in latter and former respectively.

Finally, the computational performance of the proposed RSC-MPC in each time interval for *Case IV* is summarised in Table III. This table shows the efficiency of the proposed method in terms of processing time. Besides, the considerably small value of relative gap shows the optimality and accuracy of the model.

VI. CONCLUSIONS

This paper proposed a hierarchical tri-layer min-max-min MPC framework for real-time energy scheduling of IMGs under the influence of uncertainty and real-time time-varying contingency conditions. A mathematical model is developed for inclusion of convex security constraints, allowing the real-time tracking of contingency conditions based on the geographical structure of IMG. The risk associated with the uncertainty of predicted data is also added to the proposed RSC-MPC through adapting the CVaR method in the control mechanism. A convex network reconfiguration is adopted as a corrective security measure to deal with critical line outages and risk of uncertainty on a real-time basis. The optimisation problem investigates the role of risk and time-varying security constraints in the optimal operation of IMGs. The multi-objective economic analysis of the model shows the necessity of additional budget to be considered for dealing with risk and security measures. The results show the variation of contingency condition over different zones and for various scenarios of RES uncertainty, demonstrating the necessity of a real-time approach that accounts for these measures. Furthermore, the efficiency of the proposed corrective network reconfiguration is evident in the results, such that the configuration of the system has been changed to satisfy different economic and security goals. Sensitivity analysis of risk measures and economic targets shows a considerable rise in the energy procurement cost to achieve a higher layer of risk aversion degree. Finally, the computational efficiency of the model is demonstrated by a considerably small value of relative gap.

REFERENCES

[1] J. Bialek, "What does the GB power outage on 9 August 2019 tell us about the current state of decarbonised power systems?" *Energy Policy*, vol. 146, p. 111821, 2020.

[2] M.-A. Nasr, E. Nasr-Azadani, H. Nafisi, S. H. Hosseinian, and P. Siano, "Assessing the effectiveness of weighted information gap decision theory integrated with energy management systems for isolated microgrids," *IEEE Transactions on Industrial Informatics*, vol. 16, no. 8, pp. 5286–5299, 2019.

[3] S. Nikkhah, A. Allahham, M. Royapoor, J. W. Bialek, and D. Giaouris, "Optimising building-to-building and building-for-grid services under uncertainty: A robust rolling horizon approach," *IEEE Transactions on Smart Grid*, 2021.

[4] U. R. Nair and R. Costa-Castelló, "A model predictive control-based energy management scheme for hybrid storage system in islanded microgrids," *IEEE access*, vol. 8, pp. 97 809–97 822, 2020.

[5] M. Falahi, K. Butler-Purry, and M. Ehsani, "Dynamic reactive power control of islanded microgrids," *IEEE Transactions on Power Systems*, vol. 28, no. 4, pp. 3649–3657, 2013.

[6] Q. Wu, M. Shahidehpour, C. Li, S. Huang, W. Wei *et al.*, "Transactive real-time electric vehicle charging management for commercial buildings with pv on-site generation," *IEEE Transactions on Smart Grid*, vol. 10, no. 5, pp. 4939–4950, 2018.

[7] S. Nikkhah, M. A. Nasr, and A. Rabiee, "A stochastic voltage stability constrained ems for isolated microgrids in the presence of pevs using a coordinated uc-opf framework," *IEEE Transactions on Industrial Electronics*, 2020.

[8] D. R. Prathapaneni and K. P. Detroja, "An integrated framework for optimal planning and operation schedule of microgrid under uncertainty," *Sustainable Energy, Grids and Networks*, vol. 19, p. 100232, 2019.

[9] A. Khodaei, "Resiliency-oriented microgrid optimal scheduling," *IEEE Transactions on Smart Grid*, vol. 5, no. 4, pp. 1584–1591, 2014.

[10] P. M. de Quevedo, J. Contreras, A. Mazza, G. Chicco, and R. Porumb, "Reliability assessment of microgrids with local and mobile generation, time-dependent profiles, and intraday reconfiguration," *IEEE Transactions on Industry Applications*, vol. 54, no. 1, pp. 61–72, 2017.

[11] N.-M. Zografou-Barredo, C. Patsios, I. Sarantakos, P. Davison, S. L. Walker, and P. C. Taylor, "Microgrid resilience-oriented scheduling: A robust misocp model," *IEEE Transactions on Smart Grid*, vol. 12, no. 3, pp. 1867–1879, 2020.

[12] J. D. Lara, D. E. Olivares, and C. A. Canizares, "Robust energy management of isolated microgrids," *IEEE Systems Journal*, vol. 13, no. 1, pp. 680–691, 2018.

[13] M. Singh. (Feb 2021) 'california and texas are warnings': blackouts show us deeply unprepared for the climate crisis. [Online]. Available: https://www.theguardian.com/environment/2021/feb/19/power-outages-texas-california-climate-crisis

[14] K. A. Saleh, H. H. Zeineldin, and E. F. El-Saadany, "Optimal protection coordination for microgrids considering n −1 contingency," *IEEE Transactions on Industrial Informatics*, vol. 13, no. 5, pp. 2270–2278, 2017.

[15] M. Amirioun, F. Aminifar, and H. Lesani, "Resilience-oriented proactive management of microgrids against windstorms," *IEEE Transactions on Power Systems*, vol. 33, no. 4, pp. 4275–4284, 2017.

[16] W. Sun, S. Ma, I. Alvarez-Fernandez, A. Golshani *et al.*, "Optimal self-healing strategy for microgrid islanding," *IET Smart Grid*, vol. 1, no. 4, pp. 143–150, 2018.

[17] A. A. Eajal, A. H. Yazdavar, E. F. El-Saadany, and K. Ponnambalam, "On the loadability and voltage stability of islanded ac–dc hybrid microgrids during contingencies," *IEEE Systems Journal*, vol. 13, no. 4, pp. 4248–4259, 2019.

[18] F. H. Aghdam, J. Salehi, and S. Ghaemi, "Contingency based energy management of multi-microgrid based distribution network," *Sustainable Cities and Society*, vol. 41, pp. 265–274, 2018.

[19] S. Córdova, C. Cañizares, Á. Lorca, and D. E. Olivares, "An energy management system with short-term fluctuation reserves and battery degradation for isolated microgrids," *IEEE Transactions on Smart Grid*, 2021.

[20] W. Mendieta and C. A. Cañizares, "Primary frequency control in isolated microgrids using thermostatically controllable loads," *IEEE Transactions on Smart Grid*, vol. 12, no. 1, pp. 93–105, 2020.

[21] D. K. Dheer, O. V. Kulkarni, S. Doolla, and A. K. Rathore, "Effect of reconfiguration and meshed networks on the small-signal stability margin of droop-based islanded microgrids," *IEEE Transactions on Industry Applications*, vol. 54, no. 3, pp. 2821–2833, 2018.

[22] S. Nikkhah, K. Jalilpoor, E. Kianmehr, and G. B. Gharehpetian, "Optimal wind turbine allocation and network reconfiguration for enhancing resiliency of system after major faults caused by natural disaster considering uncertainty," *IET Renewable Power Generation*, vol. 12, no. 12, pp. 1413–1423, 2018.

[23] E. Dall'Anese and G. B. Giannakis, "Risk-constrained microgrid reconfiguration using group sparsity," *IEEE Transactions on Sustainable Energy*, vol. 5, no. 4, pp. 1415–1425, 2014.

[24] M. Dabbaghjamanesh, A. Kavousi-Fard, and S. Mehraeen, "Effective scheduling of reconfigurable microgrids with dynamic thermal line rating," *IEEE Transactions on Industrial Electronics*, vol. 66, no. 2, pp. 1552–1564, 2018.

[25] P. Akaber, B. Moussa, M. Debbabi, and C. Assi, "Automated post-failure service restoration in smart grid through network reconfiguration in the presence of energy storage systems," *IEEE Systems Journal*, vol. 13, no. 3, pp. 3358–3367, 2019.

[26] A. Arif, Z. Wang, J. Wang, and C. Chen, "Power distribution system outage management with co-optimization of repairs, reconfiguration, and dg dispatch," *IEEE Transactions on Smart Grid*, vol. 9, no. 5, pp. 4109–4118, 2017.

[27] B. V. Solanki, A. Raghurajan, K. Bhattacharya, and C. A. Cañizares, "Including smart loads for optimal demand response in integrated energy management systems for isolated microgrids," *IEEE Transactions on Smart Grid*, vol. 8, no. 4, pp. 1739–1748, 2015.

[28] A. C. Luna, N. L. Diaz, M. Graells, J. C. Vasquez, and J. M. Guerrero, "Mixed-integer-linear-programming-based energy management system for hybrid pv-wind-battery microgrids: Modeling, design, and experimental verification," *IEEE Transactions on Power Electronics*, vol. 32, no. 4, pp. 2769–2783, 2016.

[29] I. Sarantakos, D. M. Greenwood, J. Yi, S. R. Blake, and P. C. Taylor, "A method to include component condition and substation reliability into distribution system reconfiguration," *International Journal of Electrical Power & Energy Systems*, vol. 109, pp. 122–138, 2019.

[30] Global Power System Transformation. Inaugural research agenda. [Online]. Available: https://globalpst.org/

[31] D. E. Olivares, A. Mehrizi-Sani, A. H. Etemadi, C. A. Cañizares, R. Iravani, M. Kazerani, A. H. Hajimiragha, O. Gomis-Bellmunt, M. Saeedifard, R. Palma-Behnke *et al.*, "Trends in microgrid control," *IEEE Transactions on smart grid*, vol. 5, no. 4, pp. 1905–1919, 2014.

[32] D. E. Olivares, C. A. Cañizares, and M. Kazerani, "A centralized energy management system for isolated microgrids," *IEEE Transactions on smart grid*, vol. 5, no. 4, pp. 1864–1875, 2014.

[33] A. Rabiee, A. Soroudi, and A. Keane, "Risk-averse preventive voltage control of ac/dc power systems including wind power generation," *IEEE Transactions on Sustainable Energy*, vol. 6, no. 4, pp. 1494–1505, 2015.

[34] G. S. Georgiou, P. Christodoulides, and S. A. Kalogirou, "Real-time energy convex optimization, via electrical storage, in buildings–a review," *Renewable Energy*, vol. 139, pp. 1355–1365, 2019.

[35] R. A. Jabr, R. Singh, and B. C. Pal, "Minimum loss network reconfiguration using mixed-integer convex programming," *IEEE Transactions on Power systems*, vol. 27, no. 2, pp. 1106–1115, 2012.

[36] M. Farrokhabadi, C. A. Cañizares, and K. Bhattacharya, "Unit commitment for isolated microgrids considering frequency control," *IEEE Transactions on Smart Grid*, vol. 9, no. 4, pp. 3270–3280, 2016.

[37] D. M. Ward, "The effect of weather on grid systems and the reliability of electricity supply," *Climatic Change*, vol. 121, no. 1, pp. 103–113, 2013.

[38] M. Kendon, "Storm malik and storm corrie, january 2022," https://www.metoffice.gov.uk/binaries/content/assets/metofficegovuk/pdf/weather/learn-about/uk-past-events/interesting/2022/2022_01_storms_malik_corrie.pdf, 2022.

[39] G. McClure, S. Langlois, and J. Rogier, "Understanding how overhead lines respond to localized high intensity wind storms," in *Structures Congress 2008: Crossing Borders*, 2008, pp. 1–10.

[40] Z. Li, S. Jazebi, and F. De Leon, "Determination of the optimal switching frequency for distribution system reconfiguration," *IEEE Transactions on Power Delivery*, vol. 32, no. 4, pp. 2060–2069, 2016.

[41] A. Kavousi-Fard, A. Zare, and A. Khodaei, "Effective dynamic scheduling of reconfigurable microgrids," *IEEE Transactions on Power Systems*, vol. 33, no. 5, pp. 5519–5530, 2018.

[42] N. G. Paterakis, A. Mazza, S. F. Santos, O. Erdinç, G. Chicco, A. G. Bakirtzis, and J. P. Catalão, "Multi-objective reconfiguration of radial distribution systems using reliability indices," *IEEE Transactions on Power Systems*, vol. 31, no. 2, pp. 1048–1062, 2015.

Saman Nikkhah (GSM'20) received the M.Sc. (Hons.) degree from the University of Zanjan, Zanjan, Iran, in 2016. He is currently pursuing the Ph.D. degree with the the School of Engineering, Newcastle University, Newcastle upon Tyne, UK. His research interests include active buildings, integrated energy systems, smart grid, resilience, and voltage stability. He has been a member of Iran National Elites Foundation since 2018.

Ilias Sarantakos received the Dipl. Ing. degree from the School of Electrical and Computer Engineering, National Technical University of Athens, Greece, in 2013, and the Ph.D. degree from the School of Engineering, Newcastle University, UK, in 2019. Since 2018 he has been a Postdoctoral Researcher with the Electrical Power Research Group, Newcastle University. His research interests include distribution network operation and planning, optimization, reliability, and security of supply

Natalia-Maria Zografou-Barredo is an EPSRC Doctoral Prize Fellow in the School of Engineering in Newcastle University, U.K. She received the Ph.D. degree in Electrical and Electronic Engineering from the School of Engineering, Newcastle University, U.K in 2022, and the Diploma degree from the Department of Electrical and Computer Engineering, School of Engineering, University of Patras, Greece in 2016. She was awarded the 2016 IEEE Greece Power and Energy Society POWERED Award (16th Workshop on Power Engineering Dissertations). Her research interests include distribution network operation, active network management, and mathematical optimization.

Abbas Rabiee (Senior Member, IEEE) received the Ph.D. degree in electrical engineering from Sharif University of Technology, Tehran, Iran, in 2013. He is currently an Associate Professor with Electrical and Electronic Engineering Department, University of Zanjan, Zanjan, Iran. His research interests include power system operation and security, renewable energies, integrated energy systems, and optimization methods. He has been awarded the 2019 Premium Award for Best Paper in IET Generation, Transmission, and Distribution.

Adib Allahham received the B.S. degree in Electric Engineering from Damascus University, Syria, and the M.Sc. and Ph.D. degrees from the Joseph Fourier University of Grenoble, France, in 2004 and 2008, respectively. From 1999 to 2003, he worked at the energy industry. In 2008, he joined the G-SCOP Laboratory, France, as a Postdoctoral Researcher. From 2009 to June 2016, he worked as a Senior Lecturer with the Electrical Power Engineering Department, Damascus University. Since 2016, he has been a Researcher with the School of Engineering, Newcastle University. He has published more than 30 peer-reviewed journal and international conference papers. His research interests include the energy storage systems, smart grid technologies, grid connected renewable energy sources, and multi-vector energy integration.

Damian Giaouris received the B.Eng. degree in automation engineering from the Technological Educational Institute of Thessaloniki, Thessaloniki, Greece, in 2000, the B.Sc. degree and Postgraduate Certificate in Mathematics from Open University, Milton Keynes, UK, in 2009 and 2011, respectively, and the M.Sc. and Ph.D. degrees in the area of control of electrical systems from Newcastle University, Newcastle upon Tyne, UK, in 2001 and 2004, respectively. He was a Lecturer in Control Systems with Newcastle University, since 2004, before moving to the Centre for Research and Technology Hellas (Greece), in 2011. Since September 2015, he has been a Senior Lecturer in Control of Electrical Systems and a Reader of Control of Energy Systems with Newcastle University. His research interests include control of power converters, power systems, smart grids, electric vehicles, and nonlinear dynamics of electrical systems. He has been in various editorial boards and has more than 150 publications.